Article

Asymmetric Spray Characteristics According to Y-Jet Nozzle Orifice Shape and Spray Conditions

Sang Ji Lee, Ji Yeop Kim, and Jung Goo Hong*

Read Online

| ACCESS | Metrics & More | Article Recommendations |

ABSTRACT: The Y-jet nozzle is a twin-fluid nozzle that has a larger operating range and simpler structure than other twin-fluid nozzles. Furthermore, it offers outstanding atomization quality even at low flow rates, mak ing it simple to atomize viscous liquids. However, because of the structure of the Y-jet nozzle, having an asymmetrical spray pattern is limited. Most existing experimental studies focused on the orifice diameter and mixing tube length. In this study, two types of elliptical nozzles and one type of circular nozzle were tested. We found that the elliptical nozzle's asymmetric spray characteristics are different from those of the circular type. Furthermore, it was demonstrated that the spray characteristics were different even in ellipsoids, with only the major and minor axes differing.

Assist air pressure 15bar (GLR: 0.11) Assist air pressure 20bar (GLR: 0.16)
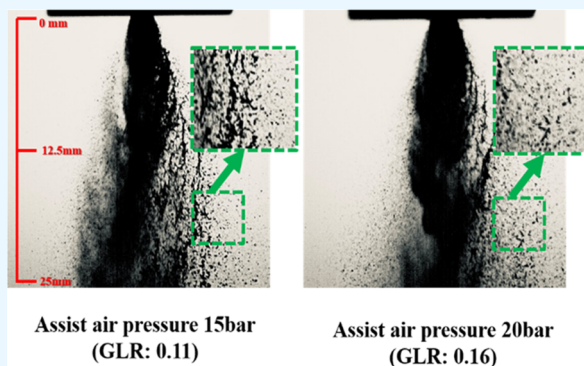
1. INTRODUCTION

When a liquid is atomized into many droplets, its overall surface area increases, and chemical processes such as heat, mass transfer, and combustion become active. A spray nozzle is commonly used for droplet atomization.[1,2] The atomizing nozzle atomizes the liquid using pressure, although it can also be achieved under air-assist, rotational, or other energy sources. The twin-fluid nozzle, in particular, increases liquid atomization by utilizing an auxiliary gas that aids in liquid atomization.[3−5] Twin-fluid nozzles have mostly been employed in industries such as industrial boilers, blast furnaces, and agricultural sprays owing to these advantages.[6] Recent applications include selective catalytic reduction (SCR) injectors, the production of microparticles, and deposition techniques in the fields of biology and pharmaceuticals.[7−10]

The Y-jet nozzle is a representative twin-fluid nozzle that can achieve the same spraying effect with a wider operating range and lower spraying pressure than pressure spraying nozzles. Furthermore, compared with other twin-fluid nozzles, it has a simple structure, and the atomization quality is excellent, even at low flow rates. Therefore, it can be used for both low- and high-viscosity solutions.[11,12] However, optimization of the nozzle design and experimental study on the spray characteristics based on the fluid supply ratio are necessary to ensure that the Y-jet nozzle can be used in various applications.

In a study by Mullinger et al.[13] on nozzle design, researchers found that the momentum of twin fluids, the ratio of the length of the mixing tube to the orifice diameter, the angle between the fuel supply tube and the auxiliary gas supply tube, and other geometric variables of the Y-jet nozzle affect the spray.

Pacifico et al.[14] demonstrated a two-phase flow that changes depending on the geometrical parameters of the Y-jet nozzle and reported that the internal flow pattern affects the external spray. According to Andreussi et al.,[15] splitting and cohesion of twin fluids in the mixing tube where the twin fluids are mixed inside the nozzle affect the external spray. Song et al.[16] investigated the asymmetric spray characteristics of the Y-jet nozzle based on the length of the mixing tube and proposed a change in the resistance of the two-phase flow in the mixing tube. Furthermore, the internal flow pattern was predicted based on this.[17]

In terms of studies on the supply ratio of twin fluids, Wigg et al.[18] stated that the gas flow rate can be maintained by preserving the injection pressure ratio of liquid and gas. It is feasible to achieve energy saving in the process using optimal injection pressure parameters. Bryce et al.[19] confirmed that the gas injection flow rate decreased as the liquid pressure increased. This means that the liquid and gas flow rates are diametrically opposed. Lee[20] asserted that asymmetric atomization of Y-jet nozzles can be minimized based on the gas-to-liquid mass flow rate (GLR). Nazeer et al.[21] developed a GLR-based mathematical analysis model of internal flow. This was also used to evaluate the asymmetric spray pattern according to

the GLR.[22] Zhou et al.[23] conducted an experimental study on a Y-jet nozzle and reported a better internal flow pattern by predicting the droplet size distribution according to the GLR.

It is essential to consider the internal flow mechanism of the fluids since a twin-fluid nozzle has a two-phase flow. Mixing two fluids within the mixing tube has a significant effect on external flow. Therefore, this requires extensive research. However, most existing studies focused exclusively on the length of the mixing tube, and only a few studies focused on the mixing tube and orifice shapes. It is considered that the shape of the mixing tube affects the development of the internal flow and hence the atomization quality of the external flow.

The purpose of this study is to compare the existing circular Y-jet internal mixing tube and the elliptical internal mixing tube. The spray characteristics of the nozzle, which determine the shape of the internal mixing tube, were obtained using a laboratory-scale Y-jet nozzle spray experimental setup. To determine the effect of GLR in an elliptical mixing tube, we evaluated the spatial spray features by comparing the droplet sizes along the X and Y axes, considering the spray shape and asymmetric spray characteristics of the Y-jet nozzle.

2. RESULTS AND DISCUSSION

2.1. GLR According to Liquid Pressure. Figure 1 shows the GLR as a function of liquid pressure for three different types of experimental nozzles. The experiment in Figure 1 (a) was carried out by increasing the liquid pressure from 0.5 to 5 bar while keeping the assist gas pressure constant at 5 bar. The mass flow of liquid increases as the liquid pressure increases, whereas the mass flow of assist gas decreases. As a result, the GLR tends to decrease.[16,17] The difference in the GLR reduction was validated at this point based on the shape of the nozzle orifice.

Under the same liquid pressure conditions, the GLR was lower in the elliptical nozzle than in the circular nozzle. This indicates that an elliptical orifice nozzle discharges less mass flow than a circular orifice nozzle under the same assist gas pressure, depending on the shape of the nozzle's exit orifice.

The variations in the assist gas mass flow rate are attributable to the difference in the orifice circumference, despite the fact that the exit orifice area is the same. Equation 1 was used to compute the circumference of the three nozzles. The circumferential difference between an elliptical orifice nozzle and a circular orifice nozzle is approximately 12%. Therefore, in the case of assist gas in an elliptical orifice nozzle, the area where the shear stress inside the nozzle's mixing tube operates is considerable, and the frictional force between the assist gas and the inner wall of the mixing tube is greater than that in the case of a circular nozzle.[24] As a result, it is determined that the same level of assist gas mass flow as the prototype is released only at a higher pressure.

$$P = \pi \sqrt{2(a^2 + b^2)} \tag{1}$$

where P is the circumference of an ellipse, a is the radius of the major axis, and b is the radius of the minor axis.

The mass flow rate of the assist gas in the mixing tube inside the nozzle has a stronger effect on atomization than the pressure of the assist gas in the internal mixing type twin-fluid nozzle. Inside the mixing tube, where there is limited space, liquid exhibits minimal variations in mass flow rate as a function of pressure, whereas the density of the assist gas is
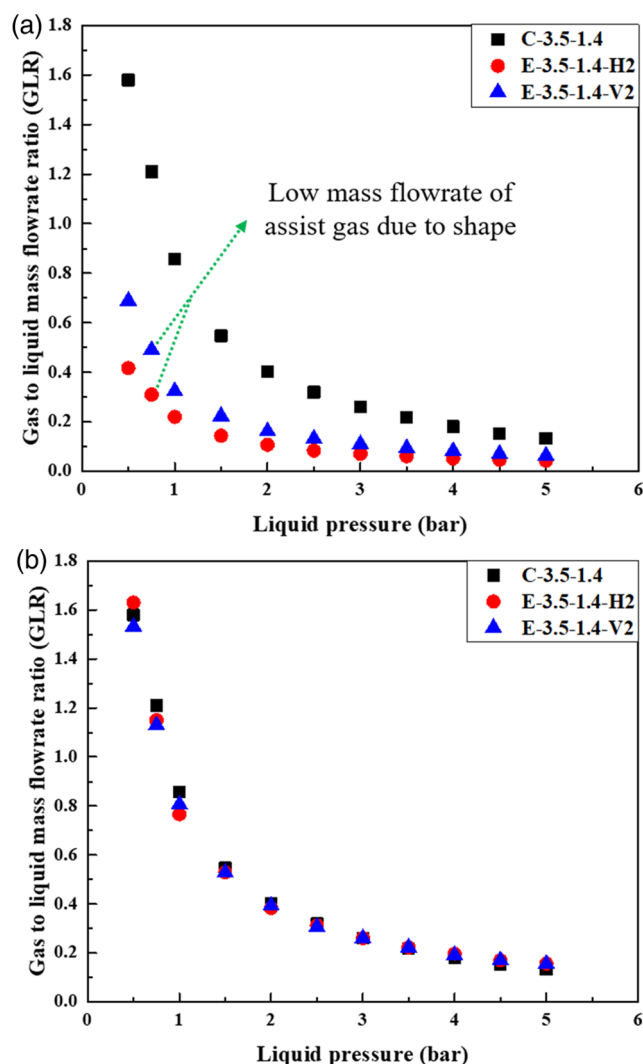

Figure 1. (a) GLR according to liquid pressure (assist gas pressure 5 bar). (b) GLR according to liquid pressure (assist gas mass flow rate same condition).

approximately 800 times lower than that of the liquid. Therefore, even when the same pressure is applied, the mass flow rate varies. As a result, the same GLR must be set within the nozzle mixing tube.

Consequently, because GLR has a significant effect in defining the Sauter mean diameter (SMD) level of the Y-jet nozzle in this study, the GLR value was changed by adjusting the assist gas pressure of each nozzle differently depending on the liquid pressure, as shown in Figure 1(b).

Figure 2 shows SMD according to GLR for three different types of experimental nozzles. The SMD measurement was conducted under the FV condition in Figure 18. The Z-axis was measured 200 mm downstream from the nozzle tip, and the X-axis was only measured at the nozzle tip's center (X-axis 0 mm). The GLR on the graph's X-axis denotes a condition in which the liquid pressure is decreased by 0.5 bar from 5 to 0.5 bar, and the assist gas mass flow rate is adjusted for each nozzle based on the liquid mass flow rate.

The test demonstrated that when the GLR increased, the SMD decreased in all three types of nozzles. This is because, as the GLR increases, the mass flow rate of the assist gas exceeds the mass flow rate of the liquid. According to the nozzle
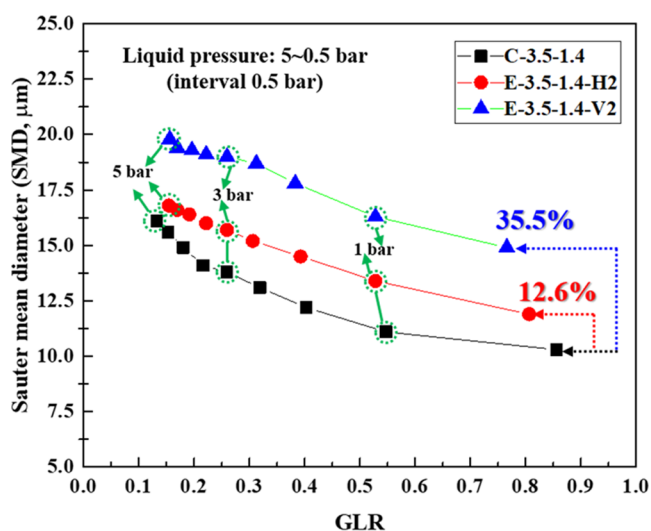
Figure 2. SMD according to GLR (liquid pressure 5−0.5 bar).

difference in SMD, the circular orifice nozzle, the C-3.5-1.4(C) nozzle, had the least SMD. Under the overall GLR condition, the E-3.5-1.4-H2(H2) nozzle had a 12.6% higher average SMD than the circular and elliptical orifice nozzles. It was confirmed that the E-3.5-1.4-V2(V2) nozzle was 35.5% larger than the original shape. It is considered that this is because the shape of the outlet orifice affects mixing in the nozzle mixing tube despite having the same mass flow rate.

Figure 3 shows the SMD distribution according to GLR. The SMD was measured more than 100 times for each nozzle under varying GLR conditions. The SMD decreases as GLR increases for all three types of nozzles, as shown in Figure 2. However, the SMD varied according to the GLR, depending on the nozzle. In the case of a circular nozzle, the variation in the SMD is the lowest when the GLR is the same. However, even the same GLR leads to variations in the SMD in the case of an elliptical nozzle. Furthermore, it was established that the saturation of SMD based on an increase in GLR was fastest for a circular nozzle and slowest for V2. When compared with the circular nozzle, the elliptical nozzle did not produce sufficient mixing between the twin fluids in the mixing tube. As a result, the elliptical nozzle had a higher SMD deviation according to the GLR than the circular nozzle. SMD of 30 μm or less was attained at a GLR of 0.4 or greater regardless of the nozzle orifice shape.[21,22] Even with a higher supply of assist gas, the effect of droplet splitting was verified to be minimal.

2.2. SMD According to the Orifice Shape of the Y-Jet Nozzle in the *Y*-Axis Radial Direction. Figures 4−6 show the SMDs along the *Y*-axis radial direction. The liquid pressures of all three types of nozzles were 1, 3, and 5 bar, respectively. The experiment was conducted with the assist gas pressure set differently and the assist gas mass flow rate set to the same level to compare the GLRs at almost the same level according to the nozzle. In Figure 18, the nozzle position in the *Y*-axis radial direction was designated as RV.

The average value was determined after measuring more than 20 times at 5 mm intervals within the *Y*-axis radius of ±20 mm around the nozzle orifice. The SMD value increased in the radial direction from 0 mm on the *Y*-axis, which is the center of the nozzle, as shown in Figures 4−6.

This is because droplet coalescence subsequently occurs as the droplets emitted from the nozzle migrate in the radial
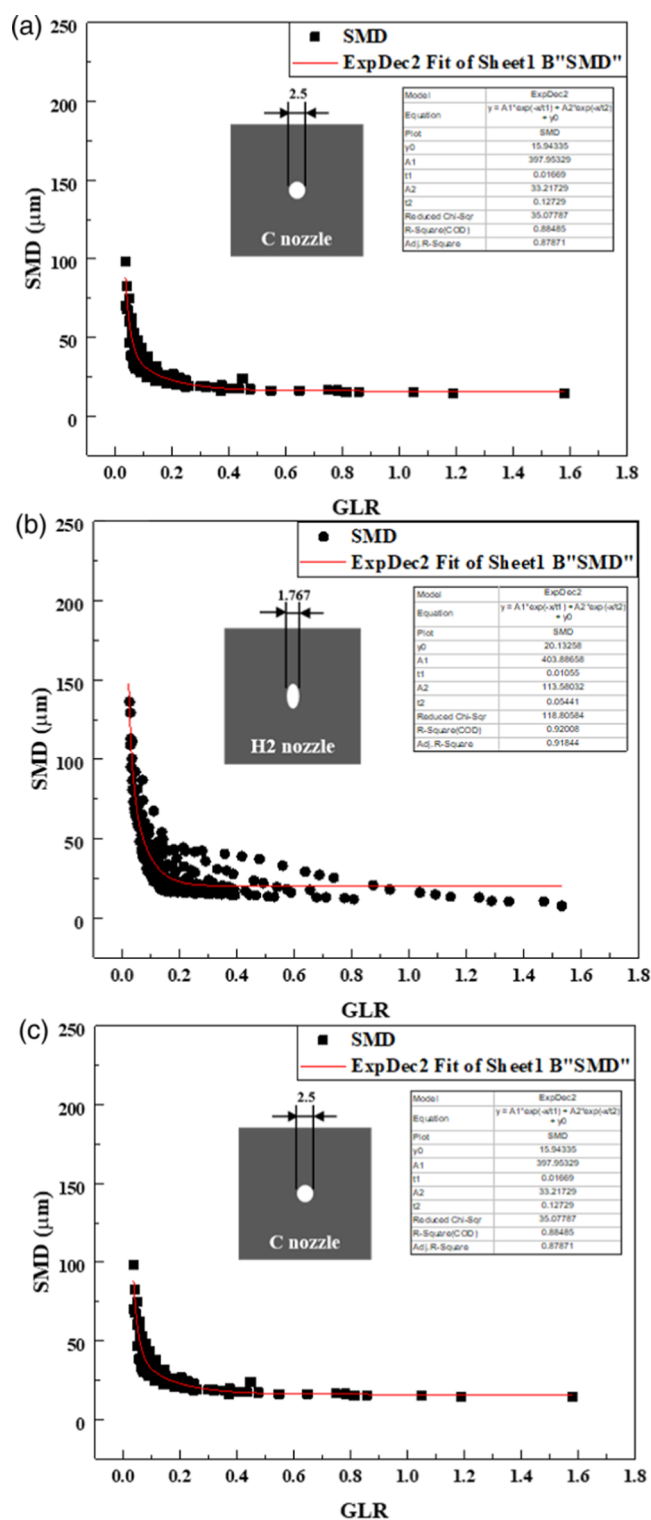

Figure 3. (a) SMD according to GLR (C-3.5-1.4). (b) SMD according to GLR (E-3.5-1.4-H2). (c) SMD according to GLR (E-3.5-1.4-V2).

direction. This is more common in circular orifice nozzles than in elliptical orifice nozzles. It is considered that the smaller the GLR, the slower the atomization develops, resulting in the difference in the radial droplet size.

Furthermore, as the GLR increased, the SMD along the *Y*-axis radial direction decreased regardless of the nozzle, and the spray asymmetry also decreased. This is because, at a high
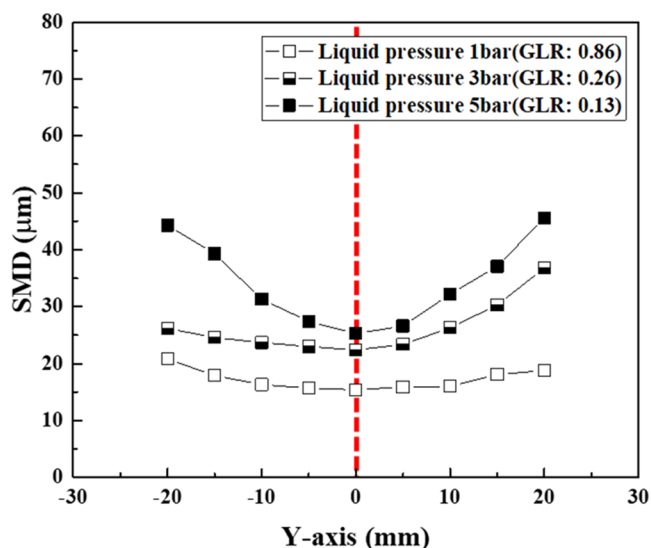
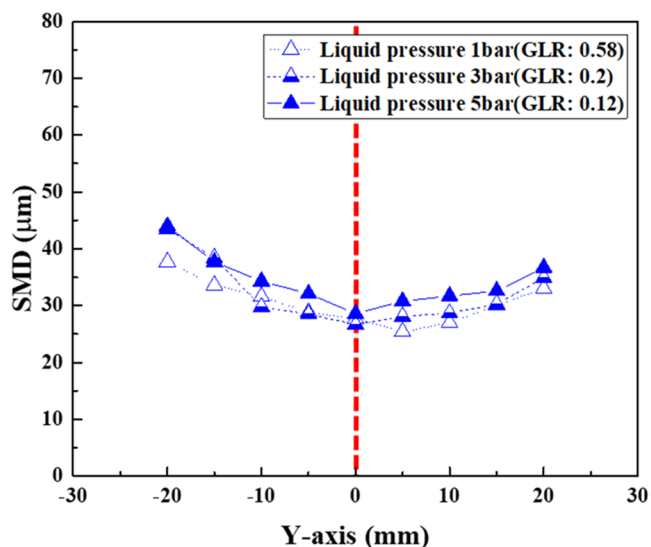**Figure 4.** SMD according to *Y*-axis (C-3.5-1.4).

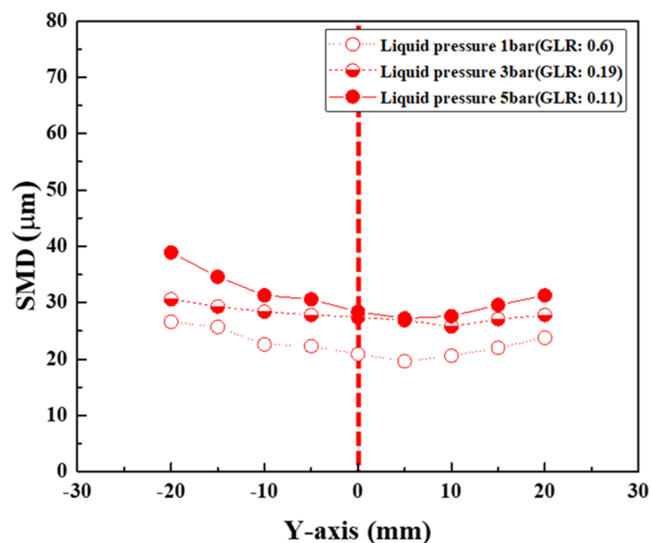**Figure 5.** SMD according to *Y*-axis (E-3.5-1.4-V2).

Figure 6. SMD according to *Y*-axis (E-3.5-1.4-H2).

GLR, the ratio of the assist gas mass flow rate is greater than the ratio of the liquid mass flow rate, indicating that atomization has progressed sufficiently.

2.3. Spray Mode SMD Standard Deviation According to Flow Rate. Figures 7−9 show the SMDs along the *X*-axis
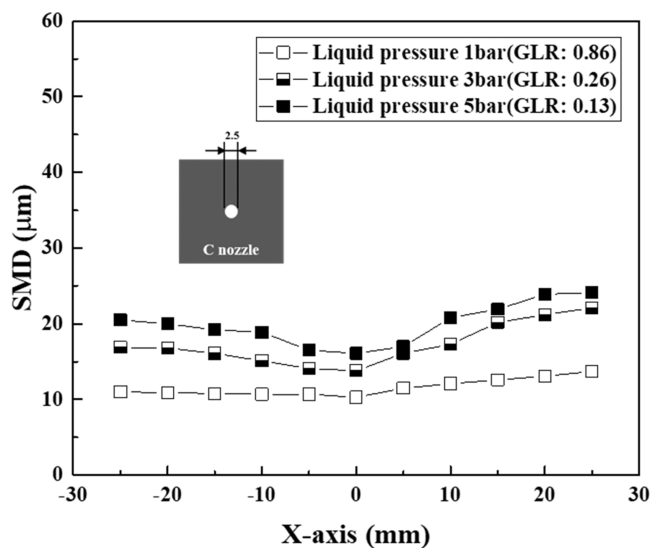

Figure 7. SMD according to *X*-axis (C-3.5-1.4).

radial direction. The liquid pressure and assist gas mass flow rate were measured under the same conditions as in Figures 4−6. The *X*-axis radial direction was measured after positioning the nozzle and SMD measuring apparatus in the FV direction of Figure 18. The average value was determined after measuring more than 20 times at 5 mm intervals within the *Y*-axis radius of ±25 mm around the nozzle orifice.

The direction in which liquid flows from the nozzle is the + direction based on the *X*-axis 0 mm, which is the center of the nozzle. Asymmetric spraying occurred along the *X*-axis radial direction, as confirmed by the experimental results. It was verified that the asymmetry was considerably more severe in the elliptical orifice nozzles of Figures 8 and 9 than in the circular orifice nozzle of Figure 7. The SMD became lower,
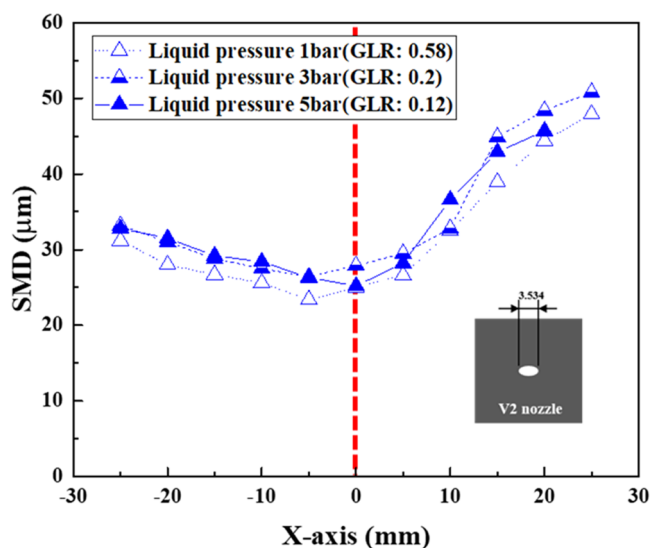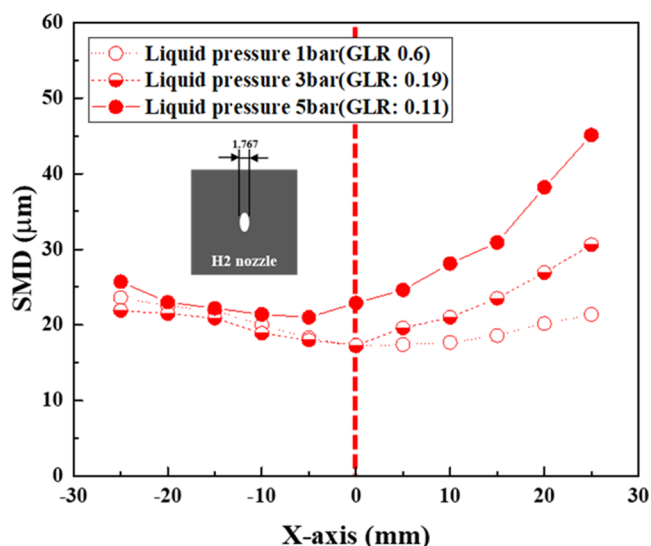

Figure 8. SMD according to *X*-axis (E-3.5-1.4-V2).

Figure 9. SMD according to *X*-axis (E-3.5-1.4-H2).

Figure 10. Schematic of the two-phase flow pattern within the mixing chamber.

and the asymmetry was attenuated when the GLR increased in the circular nozzle, as shown in Figure 7. However, it was verified that asymmetry occurred at nearly the same amount in all experimental conditions for the V2 nozzle, as shown in Figure 8. In the case of the H2 nozzle in Figure 9, it was confirmed that the asymmetry deteriorated under high liquid pressure conditions (low GLR condition).

This can be confirmed through Table 1. Table 1 is a table showing the average ratio of SMD in the + direction and SMD

Table 1. *X*-Axis Asymmetry Ratio According to Liquid Pressure

liquid pressure (bar)	C-3.5-1.4	E-3.5-1.4-V2	E-3.5-1.4-H2
1	1.16	1.39	0.89
3	1.22	1.39	1.19
5	1.12	1.34	1.45

in the − direction of the *X*-axis of Figures 7−9 according to the liquid pressure. The closer to 1, the more symmetrical the spray is. If the value is greater than 1, it is asymmetric in the + direction, and if the value is less than 1, it is asymmetric in the − direction. In the case of the C nozzle, it is 1.12−1.22 level, and in the case of the V2 nozzle, it has an asymmetry of 1.34−1.39 regardless of the pressure. On the other hand, in the case of the H2 nozzle, it does not have a value of 1.45 at 5 bar, but at 1 bar, it is 0.89, showing the result of alleviating the asymmetry. These results show a tendency consistent with previous studies on asymmetry according to GLR.[16,20−22]

Although the elliptical nozzle in Figure 8 has the same shape as that in Figure 9, the long and short axes are opposite. Despite having the same oval shape, the long and short axes are different, resulting in a different distance from the liquid entry port to the opposing wall of the mixing tube. The schematic diagram of the inside of the nozzle in Figure 10 confirms this. Even under the same GLR condition, the liquid is evenly distributed over the cross section in the left figure of Figure 10; however, it can be demonstrated that this is not the case in the right figure of Figure 10. The shorter the distance between the liquid entry port and the mixing tube wall inside the nozzle, the more equal the liquid remaining in the mixing tube is dispersed
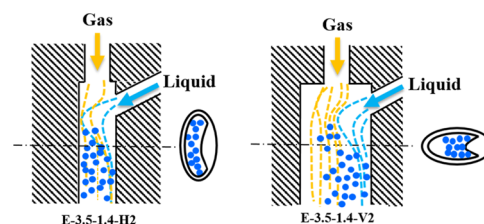
spatially. As a result, twin fluids promote the transition from bubbly flow to annular flow.

Song[17] suggested that when the GLR inside the nozzle is low, the momentum of the liquid is low, and the water sprayed from the liquid supply port does not directly contact the opposite wall. Nazeer[22] confirmed through turbulence modeling that the opposite wall was not sufficiently mixed due to the difference in momentum between the twin fluids inside the nozzle. These two researchers conducted research to reduce asymmetry through GLR, since the length from the liquid inlet to the opposite wall was the same. However, in this study, since the length from the liquid inlet to the wall is different, the internal flow in Figure 10 can be confirmed.

The V2 nozzle in Figure 8 is twice the distance from the liquid intake port to the wall of the mixing tube inside the nozzle as the H2 nozzle in Figure 9. As a result, it was determined that the twin fluids were sprayed through the outlet orifice without adequate mixing. The residence time of the twin fluids is small in the case of the H2 nozzle in Figure 9 due to the high liquid pressure under a low GLR condition; therefore, they were sprayed without being thoroughly mixed. However, the higher the GLR, the longer the residence time and the lower the asymmetry.

2.4. Asymmetric Spray Image of Y-Jet Nozzle. The spray images obtained under the experimental conditions of Figures 7−9 are shown in Figures 11−13. The spray images were obtained up to 25 mm downstream from the nozzle tip, which is approximately 10 times the diameter of the circular nozzle orifice, to validate the asymmetric spray at the start of the spray. When the liquid pressure increases, the liquid mass flow rate and water density also increase regardless of the nozzle design, and the asymmetric spray tends to worsen owing to the relatively low assist air pressure. Similar to the results in Figures 7−9, an oval nozzle produces an overall asymmetrical spray shape compared with that of a circular nozzle. In particular, it is confirmed in Figure 12 that it is asymmetric regardless of the liquid pressure. As the liquid pressure decreases, the spray shape becomes more symmetrical, as shown in Figure 13. This corresponds to the findings in Figures 8 and 9.

2.5. Y-Jet Nozzle Asymmetric Spray Characteristics According to GLR. Figure 14 shows the result of the experiment obtained by increasing the assist gas mass flow rate while the liquid pressure was fixed at 5 bar using the H2 nozzle. The other conditions are the same as those in Figure 9. In Figure 9, it was confirmed that when the assist gas mass flow rate was increased at a liquid pressure of 5 bar, the GLR increased, and the asymmetry decreased, resulting in the most asymmetric SMD result. This can be observed in the spray image in Figure 15. Although the liquid pressure is the same, the droplet size on the right side of the spray is different.
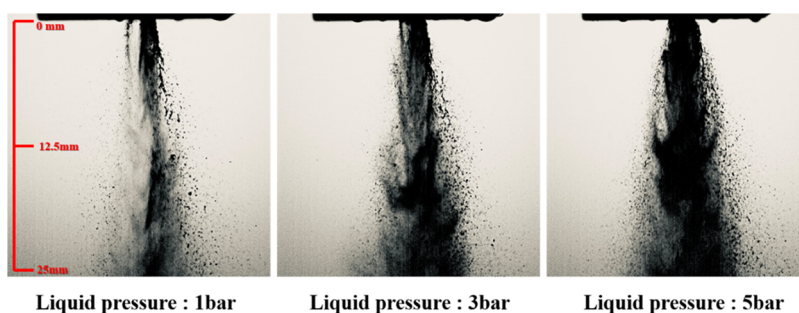
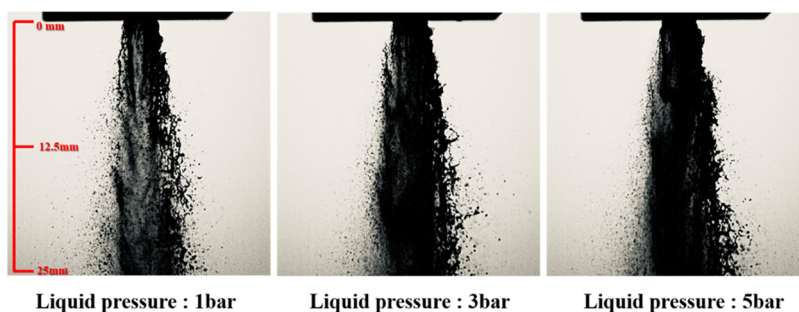**Figure 11.** Spray image according to liquid pressure (C-3.5-1.4).

Figure 12. Spray image according to liquid pressure (E-3.5-1.4-V2).
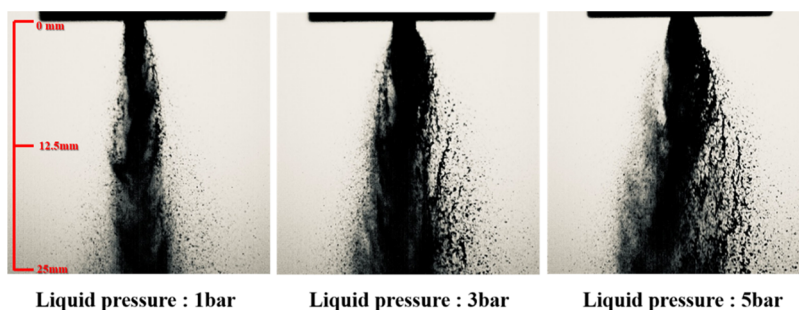

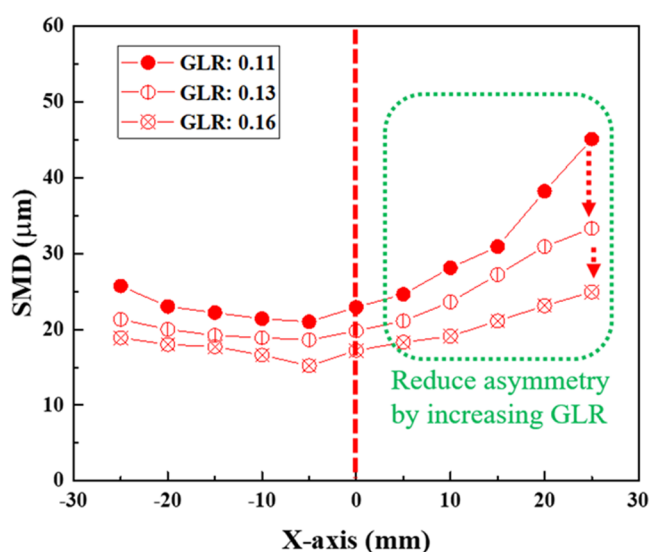**Figure 13.** Spray image according to liquid pressure (E-3.5-1.4-H2).

Figure 14. Asymmetry reduction effect according to GLR increase at liquid pressure 5 bar in Figure 9.
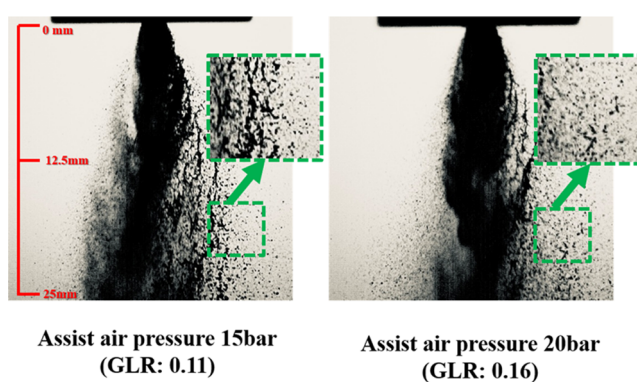

Figure 15. Image of the asymmetry reduction effect according to the increase in GLR at liquid pressure 5 bar.

The internal mixing of the twin fluids in the Y-jet nozzle affects the asymmetry. The residence time for sufficient mixing of the twin fluids in the mixing tube and the volume fraction ratio of the liquid and gas occupying the inside of the mixing tube are critical parameters that affect internal mixing. Because the flow rate was relatively fast at a liquid pressure of 5 bar in
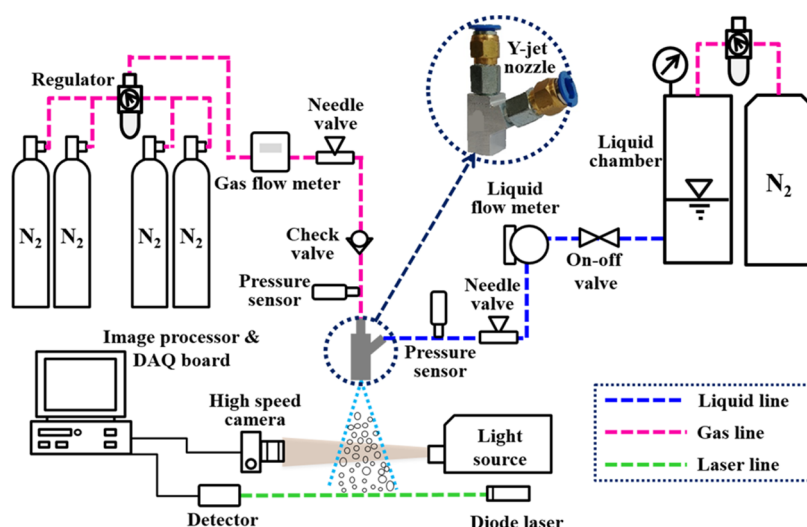
Figure 16. Experimental setup (photograph courtesy of "Sang Ji Lee," copyright 2023).

Figure 9, the asymmetry was found to be quite significant because the residence time was insufficient.

GLR encourages the evolution of twin fluids from bubbly to annular flow. If the residence time in the nozzle mixing tube is decreased because of high liquid pressure and high internal flow rate, the spraying asymmetry should be decreased by increasing the GLR.

3. CONCLUSIONS

The spatial spray characteristics of the Y-jet nozzle were observed and experimentally verified in this work based on the shape of the exit orifice.

(1). The elliptical nozzle discharged less flow than the circular nozzle under the same assist gas pressure condition. The circumference of an elliptical nozzle is approximately 12% longer than that of a circular nozzle. As a result of the increased shear stress caused by friction with the nozzle mixing tube wall, the discharge flow rate of the assist gas would become lower.

(2). The elliptical nozzle produced a more asymmetrical spray pattern than the circular nozzle under identical GLR conditions. It is considered that the internal mixing tube's shape slows down flow development.

(3). Although the V2 nozzle in which liquid flows in along the major axis had elliptical nozzles of the same shape, there was essentially no difference in the spray patterns according to the GLR. However, the asymmetry of the H2 nozzle in which liquid flows in along the minor axis decreased with an increase in GLR.

4. EXPERIMENTAL SETUP AND CONDITIONS

4.1. Experimental Setup. Figure 16 shows a schematic diagram of the laboratory-scale Y-jet nozzle spray experimental setup. The gas supply part is on the left side of the Y-jet nozzle at the center of the schematic diagram, and the liquid supply part is on the right. A measurement instrument and an image capture device are positioned below the Y-jet nozzle. The liquid was supplied through a surge tank (BT100-2J), and the surge tank was pressurized by nitrogen gas (approximately 10 bar). A nitrogen cylinder was connected in parallel to the supply gas. The supply flow rates of both fluids were regulated using an on—off valve and a needle valve and measured using a

digital flowmeter (SMC-PF2a711). The nozzle's shear pressure was measured using a pressure sensor. The real-time flow rate and pressure data were collected using a data collecting board (NI DAQ-9172, National Instruments).

The flow rate and pressure data in this experiment are the averages of sampling at 100 Hz for 10 s.[25,26] The spray image of the Y-jet nozzle was recorded by attaching a high-speed camera (Phantom VEO E310L, maximum resolution: 512 × 512, sample rate: 11,500 f/s) to the front of the nozzle and a light source to the back. Spray images were collected more than 500 times per experimental condition after ensuring that the spray pattern had attained a static state based on the spray conditions. The spray image was measured from the nozzle tip to 25 mm in the downstream of the spray direction to verify the splitting pattern at the start of spraying. As shown in Figure 17, the Sauter mean diameter (SMD) was measured using a
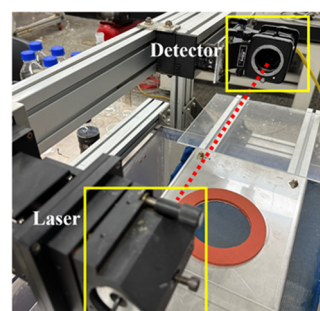

Figure 17. SMD detector system (line-up sight type) (photograph courtesy of "Sang Ji Lee," copyright 2023).

Malvern-type measuring apparatus (MLXA-A12-635-5, measuring range of approximately 8−450 μm, working distance of within 400 mm, laser spot radius of 3.9 [pixel]) and CCD (EPIX CMOS camera). The apparatus monitors the droplet size using the principle of laser diffraction and calculates the diffraction rate of the droplet captured by the laser line.[25−28] According to Mullinger et al.,[13] complete atomization was achieved downstream of the spray at approximately 40 times the diameter of the nozzle orifice. However, the SMD was measured under the condition of 200 mm downstream of the
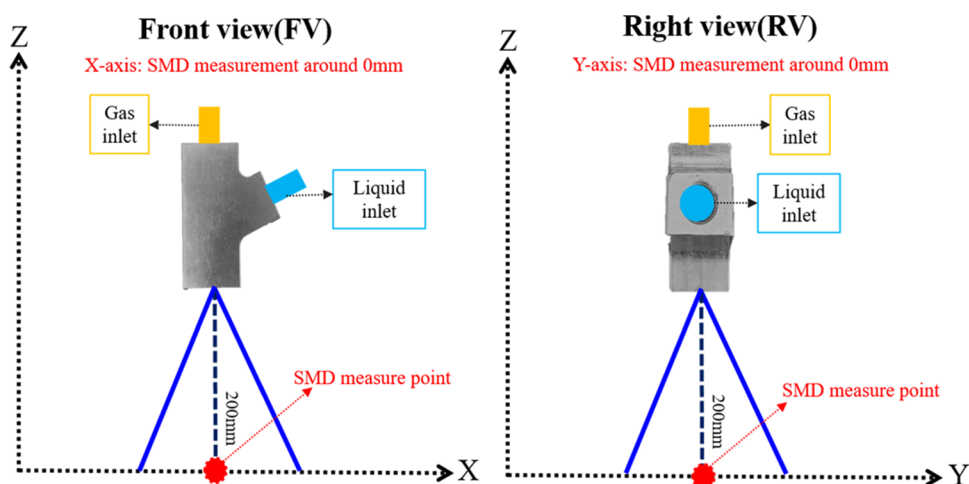
Figure 18. Y-jet nozzle arrangement according to SMD measurement direction[20] [ACS Omega/Copyright Sang Ji Lee].

spray from the nozzle tip, considering the asymmetry of the Y-jet nozzle.

Figure 18 shows a schematic diagram of the SMD measurement direction. Because the Y-jet nozzle has asymmetric spray properties, the results depend on the SMD measurement direction. Therefore, the SMD was calculated by dividing it into a front view (FV) and a right view (RV) that had been rotated by 90°. Only droplets passing through the laser line were detected because the operation of the SMD measurement instrument used in this experiment is based on the line-of-sight principle. Therefore, the nozzle's center was set at 0 mm. The SMD was measured along the X-axis radial direction at 5 mm intervals from the center of the nozzle in the front direction. The Y-axis radial direction was measured by placing the nozzle in the lateral direction and rotating it by 90°.[20]

4.2. Experimental Condition and Nozzle Design. Table 2 lists the experimental conditions. Water at ambient

Table 2. Experimental Setup

condition	value
liquid density (kg/m^3)	1000
assist gas density (kg/m^3)	1.226
liquid pressure (bar)	0.5−5
assist gas pressure (bar)	1−15
ambient temperature (°C)	20

temperature was used as the working fluid in the experiment, and nitrogen gas with a purity of 95% was used as the assist gas. Water was sprayed at pressures in the range of 0.5−5 bar, whereas nitrogen was sprayed at pressures in the range of 1−15 bar. The experiment was conducted at 0.5 bar pressure for water and 1 bar for nitrogen. Because the density of nitrogen is approximately 816 times that of water, a comparison should be performed by converting the mass flow rate rather than dealing with the injection circumstances of twin fluids via pressure. As a result, the twin fluids' mass flow rate was referred to as a nondimensionalized GLR ratio. The relational equation of GLR is given in eq 2 below.

$$GLR = \frac{\text{Liquid mass flowrate}}{\text{Assist gas mass flowrate}} \quad (2)$$

Figures 19 and 20 show the cross sections of three different types of Y-jet nozzles utilized in the experiment. Electrical
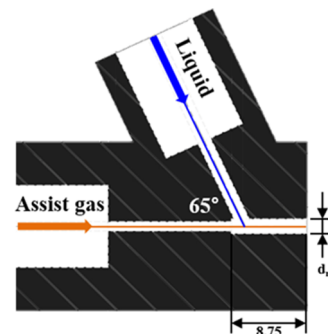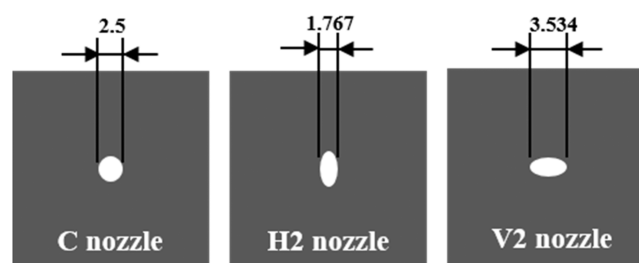

Figure 19. Nozzle design.

Figure 20. Nozzle orifice shapes.

discharge machining was used to create all three nozzles using aluminum. The twin fluids delivered into the nozzle by the liquid supply tube and auxiliary gas supply tube were mixed in the mixing tube and sprayed through the exit orifice of the Y-jet nozzle.

The specifications of the three types of nozzles utilized in the experiment are listed in Table 3. For all three nozzles, the

Table 3. Nozzle Design Factor

nozzle	major axis (mm)	minor axis (mm)	L_m (mm)	exit orifice area (mm^2)	angle (°)
C-3.5-1.4	2.5		8.75	4.906	65
E-3.5-1.4-H2	3.534	1.767		4.908	
E-3.5-1.4-V2	1.767	3.534			

diameters of the liquid supply tube and the auxiliary gas supply tube are identical. The ratio of the diameter of the liquid supply tube to that of the auxiliary gas supply tube is 1.4. In addition, the angle between the liquid and gas supply tubes is 65°, and the length of the mixing tube is 8.75 mm. The diameter of the exit orifice of the circular nozzle C-3.5-1.4(C) is 2.5 mm. In the case of two types of elliptical nozzles, it was set equal to the area of the circular nozzle's exit orifice. The major and minor axes of the E-3.5-1.4-H2(H2) and E-3.5-1.4-V2(V2) nozzles are 3.534 mm and 1.767 mm, respectively. The ratio of the main to the minor axes is 2:1, although the major and minor axes were designed to move in opposite directions.

■ AUTHOR INFORMATION

Corresponding Author

    Jung Goo Hong − *School of Mechanical Engineering, Kyungpook National University, Daegu 41566, Republic of Korea;* ⓘ orcid.org/0000-0002-1286-5728; Phone: 82-53-950-6570; Email: jghong70@knu.ac.kr; Fax: 82-53-950-6550

Authors

    Sang Ji Lee − *School of Mechanical Engineering, Kyungpook National University, Daegu 41566, Republic of Korea*

    Ji Yeop Kim − *School of Mechanical Engineering, Kyungpook National University, Daegu 41566, Republic of Korea*

Complete contact information is available at:
https://pubs.acs.org/10.1021/acsomega.3c00016

Notes

The authors declare no competing financial interest.

■ ACKNOWLEDGMENTS

■ REFERENCES

(1) Lefebvre, A. H.; McDonell, V. G. *Atomization and sprays*, 2nd ed.; Begell House: Boca Raton, USA, 2017.

(2) Sultan, F.; Ashgriz, N.; Sojka, D. R.; Guildenbecher, P. E. *Handbook of Atomization and sprays*; Springer: New York, USA, 2011.

(3) Lefebvre, A. H. Twin-Fluid Atomization: Factors Influencing Mean Drop Size. *Atomization Sprays* **1992**, *2*, 101−119.

(4) Jedelsky, J.; Jicha, M.; Slama, J.; Otahal, J. Development of an effervescent atomizer for industrial burners. *Energy Fuels* **2009**, *23*, 6121−6130.

(5) Sovani, S. D.; Sojka, P. E.; Lefebvre, A. H. Effervescent Atomization. *Prog. Energy Combust. Sci.* **2001**, *27*, 483−521.

(6) Lee, C. W.; Lee, Y. J.; Park, J. W.; Terasima, K. In *Effect of Nozzle Hole Configuration on Spray Characteristics for Diesel Engine*, 10th Annual Conference on Liquid Atomization and Spray Systems; Seoul, Korea, 2005; pp 267−272.

(7) Ye, B.; Xua, Hong.; Baoa, Binbin.; Xuanb, Jin.; Zhang, Li. 3D-printed air-blast microfluidic nozzles for preparing calcium alginate microparticles. *RSC Adv.* **2017**, *7*, 48826−48834.

(8) Kim, M. J.; Park, S. C.; Choi, S. O. Dual-nozzle spray deposition process for improving the stability of proteins in polymer micro-needles. *RSC Adv.* **2017**, *7*, 55350−55359.

(9) Su, L.; Zhang, Y.; Du, Q.; Dai, X.; Gao, J.; Dong, P.; Wang, H. An experimental study on the removal of submicron fly ash and black carbon in a gravitational wet scrubber with electrostatic enhancement. *RSC Adv.* **2020**, *10*, 5905−5912.

(10) Hejazian, M.; Darmanin, C.; Balaur, E.; Abbey, B. Mixing and jetting analysis using continuous flow microfluidic sample delivery devices. *RSC Adv.* **2020**, *10*, 15694−15701.

(11) Tanasawa, Y.; Miyasaka, Y.; Umehara, M. In *Effect of Shape of Rotating Disks and Cups on Liquid Atomization*, Proceedings of ICLASS;Tokyo, Japan, 1978; pp 165−172.

(12) Wade, R. A.; Weertes, J. M.; Gore, J. P.; Eckerle, W. A. Effervescent Atomization at Injection Pressures in the MPa Range. *Atomization Sprays* **1999**, *9*, 651−667.

(13) Mullinger, P. J.; Chigier, N. A. The design and performance of internal mixing multi jet twin-fluid atomizers. *J. Inst. Fuel* **1974**, *47*, 251−261.

(14) Pacifico, A. L.; Yanagihara, J. I. The influence of geometrical and operational parameters on Y-jet atomizers performance. *J. Braz. Soc. Mech. Sci. Eng.* **2014**, *36*, 13−22.

(15) Andreussi, P.; Tognotti, L.; Michele, G. de.; Graziadio, M. Design and characterization of twin-fluid Y-Jet atomizers. *Atomization Sprays* **1992**, *2*, 45−59.

(16) Song, S. H.; Lee, S. Y. In *An Examination of Spraying Performance of Y-Jet Atomizers Effect of Mixing Port Length*, Proceedings of ICLASS; ICLASS: Rouen, France, 1994.

(17) Song, S. H.; Lee, S. Y. Study of Atomization Mechanism of Gas/Liquid Mixtures Flowing through Y-Jet Atomizers. *Atomization Sprays* **1996**, *6*, 193−209.

(18) Wigg, L. D. Drop Size Prediction for Twin-Fluid Atomization. *J. Inst. Fuel* **1964**, *37*, 500−505.

(19) Bryce, W. B.; Cox, N. W.; Joyce, W. I. In *Oil Droplet Production and Measurement from a Twin Fluid Atomizer Using Real Fluids*, Proceeding of 1st ICLASS, 1978; pp 259−263.

(20) Lee, S. J.; Kim, J. Y.; Hong, J. G. Effects of Y-Jet Nozzle Mixing Chamber Length and the GLR on Spatial Asymmetric Spray. *ACS omega* **2021**, *6*, 16795−16803.

(21) Nazeer, Y. H.; Ehmann, M.; Koukouvinis, P.; Gavaises, M. The influence of geometrical and operational parameters on internal flow characteristics of internally mixing twin-fluid Y-jet atomizers. *Atomization Sprays* **2019**, *29*, 403−428.

(22) Nazeer, Y. H.; Ehmann, M.; Sami, M.; Gavaises, M. Atomization mechanism of internally mixing twin-fluid y-jet atomizer. *J. Energy Eng.* **2021**, *147*, No. 04020075.

(23) Zhou, Y.; Zhang, M.; Yu, J.; Zhu, X.; Peng, J. Experimental investigation and model improvement on the atomization performance of single-hole Y-jet nozzle with high liquid flow rate. *Powder Technol.* **2010**, *199*, 248−255.

(24) Hong, J. G.; Ku, K. W.; Kim, S. R.; Lee, C. W. Effect of Cavitation in Circular Nozzle and Elliptical Nozzles on the Spray Characteristic. *Atomization Sprays* **2010**, *20*, 877−886.

(25) Ku, K. W.; Hong, J. G. Thermo Fluid Effect of the Urea Thermal Decomposition in a Lab-scaled Reactor. *Chem. Eng. J.* **2015**, *264*, 625−632.

(26) Ku, K. W.; Hong, J. G.; Park, C. W. Effect of Assist-air of Twin Fluid Atomizer on Urea Thermal Decomposition. *Atomization Sprays* **2015**, *25*, 895−915.

(27) Ku, K. W.; Hong, J. G.; Park, C. W.; Chung, K. Y.; Sohn, S. H. Effect of Various Factors on the Conversion Efficiency of Urea Solution in a Urea Selective Catalytic Reduction System. *Energy Fuels* **2014**, *28*, 5959−5967.

(28) Kim, J. Y.; Lee, S. J.; Baik, G. Y.; Hong, J. G. Viscosity Effect on the Electrospray Characteristics of Droplet Size and Distribution. *ACS Omega* **2021**, *6*, 29724−29734.